CFD Letters

Journal homepage:
https://semarakilmu.com.my/journals/index.php/CFD_Letters/index
ISSN: 2180-1363

Generalized Cattaneo's Law over a Vertical Cylinder on Casson Fluids

Husna Izzati Osman[1], Dennis Ling Chuan Ching[2], Nur Fatihah Mod Omar[1], Dumitru Vieru[3], Zulkhibri Ismail[1,*]

[1] Centre for Mathematical Sciences, College of Computing and Applied Sciences, Universiti Malaysia Pahang, Lebuhraya Tun Razak, 263000 Gambang, Pahang, Malaysia
[2] Department of Fundamental and Applied Sciences, Universiti Teknologi Petronas, Seri Iskandar, 32610 Tronoh, Perak, Malaysia
[3] Department of Theoritical Mechanics (MT), Georgia Asachi Technical University of lasi TU lasi, Romania

ARTICLE INFO

Article history:
Received 6 September 2022
Received in revised form 28 September 2022
Accepted 20 October 2022
Available online 31 December 2022

Keywords:
Cattaneo; Casson fluid; Laplace transform; fractional derivative; vertical cylinder

ABSTRACT

The analysis of unsteady axial symmetric flows of an incompressible and electrically conducting Casson fluid over a vertical cylinder with time-variable temperature, under influence of an external transversely magnetic field has been carried out. The mathematical model is build based on the time-fractional differential equation of Cattaneo's law with Caputo derivative to describe thermal transport. Based on the model, we can obtain the effect of temperature gradient history on heat transport and fluid motion. Besides, the generalized mathematical model that we build can be used to achieve the Classical Cattaneo's law. Comparison between the generalized Cattaneo and the classical Cattaneo was examined to optimize the heat transport model.

1. Introduction

Non-Newtonian fluids are important in several fields of engineering applications especially in the extraction of crude oil from petroleum products such as polymer processing. Many researchers interested to study about the non-Newtonian fluids because non-Newtonian fluids has more appropriate behaviour than Newtonian [1]. Some examples of non-Newtonian fluids are butter, cheese and honey where the fluids viscosity is only dependent on temperature. Many researchers carried out their work in industrial environment on the flow of the Casson fluid with the effects on various parameter. The Casson fluid effects on magneto-hydrodynamics (MHD) unsteady heat and mass transfer free convective past an infinite vertical plate was studied by Abdullahi *et al.,* [2]. Mondal *et al.,* [3] was studied about the heat transfer behavior of viscous dissipative chemically reacted Casson fluid where the discussion was made with the impact of suction, thermal conductivity and variable viscosity in this paper.

* *Corresponding author.*
E-mail address: zulkhibri@ump.edu.my (Zulkhibri Ismail)

https://doi.org/10.37934/cfdl.14.12.3851

An interesting study was made by Aghighi *et al.,* [4] where they investigated numerically the Rayleigh-Benard Convection (RBC) in viscoplastic fluids and consider the Casson fluid in a bidimensional square cavity heated from below. Parandhama *et al.,* [5] were studied the impact of induced magnetic field on Casson fluid flow past a vertical plate. They stated that the velocity falls down with an increase of Casson fluid parameter β . Recent advancements in the study of Casson fluid flow, Ramanuja and Nagaradhika [6] were studied MHD analysis of Casson fluid through a vertical porous surface with chemical reaction. Unsteady flows of a viscous, incompressible and electrically conducting Casson fluid past a moving vertical cylinder with time-variable temperature under the impact of mass diffusion, transversely uniform magnetic field, and chemical reaction have been studied by Kumar and Rizvi [7]. Using a numerical scheme based on the Crank-Nicolson implicit finite differences, the authors analyzed fluid motion and heat and mass transfer. Some of the interesting results on Casson fluid can be found in reports by Ali and Sandeep [8], Yusof *et al.,* [9], Aman *et al.,* [10], Omar *et al.,* [11] and Daud *et al.,* [12].

The classical mathematical models of heat transport are seeming irrelevant for the recent developments in technology of measurements in heat transfer. Many researchers in the heat transfer have developed another mathematical model that are able to explain the complex phenomena of diffusion processes. Therefore, the advance mathematical models of heat transfer based on the constitutive equations with fractional derivatives in time or space have been studied and achieved.

The science of fractional derivative is quite interesting and recently many researchers presented their useful contributions on this topic. Guo *et al.,* [13] have performed the novel fractional order simulations in order to inspect the characteristics of mass and heat transfer over porous inclined surface subject to the magnetic impact. Ogunrinde *et al.,* [14] have implemented the idea of fractional simulations for the solutions of COVID-19 disease. Zhang *et al.,* [15] applied the fractional derivative scheme to present the simulations for a bio-convective problem with heat conduction model and able to predict thermal response between diffusion and wave behavior. Thakare and Warbhe [16] have discussed the time fractional thermoelastic state of a thermally sensitive functionally graded thick hollow cylinder subjected to internal heat source. Xu and Wang [17] successfully implemented analytical solution of time fractional Catteno heat equation for finite slab under pulse heat flux. Other researchers performed Cattaneo's law effects can be seen on studies by Qi *et al.,* [18], Han *et al.,* [19] and Herma and Shivakumara [20].

In this paper, we have carried out the unsteady axial symmetric flows of incompressible and electrically conducting Casson fluids over a vertical cylinder with time-variable temperature, under influence of an external transversely magnetic field. The thermal transport is described by a generalized mathematical model based on the time-fractional differential equation of Cattaneo's law with Caputo derivative. Hence, the effect of the temperature gradient on heat transport and fluid motion are able to explained by our model. The generalized mathematical model of thermal transport can be particularized to obtain the classical Cattaneo's law.

The effect of the of the temperature gradient on the thermal transport and the fluid movement has been accomplished by numerical simulations and graphic illustrations by considering the temperature of the cylindrical surface varying exponentially with time. A comparison of the two models, the generalized Cattaneo and the classic Cattaneo gives information on the optimal choice of the thermal transport model.

2. Statement of the Problem

We consider the unsteady flow of an incompressible, electrically conducting Casson fluid over a semi-infinite vertical circular cylinder of radius R_O. The $\tilde{z}$-axis of a cylindrical coordinate system $(\tilde{r}, \tilde{\varphi}, \tilde{z})$ is carry along the axis of cylinder in the vertical upward direction. The gravitational acceleration, g is in downward direction, $\vec{g} = -g\vec{e}_{\tilde{z}}$ as shown in Figure 1. Magnetic field $\vec{B} = B_0\vec{e}_{\tilde{r}}$ and $B_0 = const$ are applied to the fluid.

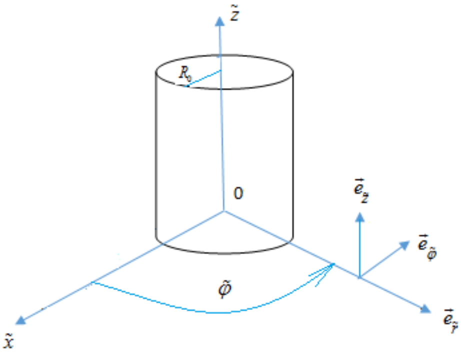

Fig. 1. Flow geometry

The rheological equation of state for Cauchy stress tensor of Casson fluid is given by

$$\tau_{ij} = \begin{cases} 2\left(\mu_B + \dfrac{P_y}{\sqrt{2\pi}}\right)e_{ij}, \pi > \pi_c \\ 2\left(\mu_B + \dfrac{P_y}{\sqrt{2\pi_c}}\right)e_{ij}, \pi > \pi_c \end{cases}, \tag{1}$$

where $\tau = (\tau_{ij})$, $i, j = 1, 2, 3$ is the shear stress tensor, $\pi = e_{ij}e_{ij}$, e_{ij} is the $(ij)^{th}$ component of the deformation rate tensor, π_c is a critical value of the product π, μ_B is a plastic dynamic viscosity of the non-Newtonian fluid,

$$P_y = \frac{\mu_B\sqrt{2\pi}}{\gamma} \tag{2}$$

where P_y denotes the yield stress of the fluid. If a shear stress less than the yield stress applied to the fluid, it behaves like a solid whereas if a shear stress greater than yield stress is applied, the fluid starts to move. Therefore, the non-Newtonian Casson fluids flow if. $\pi > \pi_c$ Denoting the dynamic viscosity,

$$\mu = \mu_B + \frac{P_y}{\sqrt{2\pi}} \tag{3}$$

we obtain the kinematic viscosity,

$$\nu = \frac{\mu}{\rho} = \frac{\mu_B + \frac{P_y}{\sqrt{2\pi}}}{\rho} = \frac{\mu_B + \frac{1}{\gamma}\mu_B}{\rho} = \frac{\mu_B}{\rho}\left(1+\frac{1}{\gamma}\right) \tag{4}$$

where ρ is the mass density and γ is called the Casson parameter.

Consider the velocity field of the form $\vec{v}\left(\tilde{r},\tilde{\varphi},\tilde{z},\tilde{t}\right) = \tilde{u}\left(\tilde{r},\tilde{t}\right)\vec{e_{\tilde{z}}}$. The fluid t emperature $\tilde{T}$ is considered as function of $(\tilde{r},\tilde{t})$, therefore $\tilde{T} = \tilde{T}\left(\tilde{r},\tilde{t}\right)$, and the heat flux vector is given by $\vec{q} = \tilde{q}(\tilde{r},\tilde{t})\vec{e_{\tilde{r}}}$. Taking into consideration the above assumption and the Boussinesq's approximation, the flow heat transfer is governed by the linear momentum equation, energy equation and Cattaneo-Vernotte's constitutive equation [1,2]:

$$\frac{\partial \tilde{u}(\tilde{r},\tilde{t})}{\partial \tilde{t}} = \nu\left(1+\frac{1}{\gamma}\right)\frac{1}{\tilde{r}}\frac{\partial}{\partial \tilde{r}}\left(\tilde{r}\frac{\partial \tilde{u}(\tilde{r},\tilde{t})}{\partial \tilde{r}}\right) + g\beta\left(\tilde{T}\left(\tilde{r},\tilde{t}\right) - \tilde{T}_\infty\right) - \frac{\sigma B_0^2}{\rho}\tilde{u}(\tilde{r},\tilde{t}) \tag{5}$$

$$\rho c_P \frac{\partial \tilde{T}(\tilde{r},\tilde{t})}{\partial \tilde{t}} = -div\vec{q} \tag{6}$$

$$\vec{q}\left(\tilde{r},\tilde{t}\right) + \tau_q \frac{\partial \vec{q}\left(\tilde{r},\tilde{t}\right)}{\partial \tilde{t}} = -k\, grad\left(\tilde{T}\left(\tilde{r},\tilde{t}\right)\right) \tag{7}$$

Where β is the thermal expansion coefficient, σ is the electrical conductivity of the fluid, c_p is the specific heat, τ_q is the thermal relaxation time and k is the thermal conductivity of the fluid. Under the velocity field assumption, we have $u_{\tilde{r}} = 0,\ u_{\tilde{\varphi}} = 0,\ u_{\tilde{z}} = \tilde{u}(\tilde{r},\tilde{t})$, therefore the continuity Eq. (5) is identically satisfied.

The divergence operator in cylindrical coordinate is $div\vec{q} = \frac{1}{\tilde{r}}\frac{\partial}{\partial \tilde{r}}(\tilde{r}q_{\tilde{r}}) + \frac{1}{\tilde{r}}\frac{\partial q_{\tilde{\varphi}}}{\partial \tilde{\varphi}} + \frac{\partial q_{\tilde{z}}}{\partial \tilde{z}}$. Since $q_{\tilde{r}} = \tilde{q}(\tilde{r},\tilde{t})$, $q_{\tilde{\varphi}} = 0$, $q_{\tilde{z}} = 0$, we obtain

$$div\vec{q} = \frac{1}{\tilde{r}}\frac{\partial}{\partial \tilde{r}}\left(\tilde{r}\tilde{q}\left(\tilde{r},\tilde{u}\right)\right). \tag{8}$$

Also, $grad\tilde{T}\left(\tilde{r},\tilde{t}\right) = \frac{\partial \tilde{T}\left(\tilde{r},\tilde{t}\right)}{\partial \tilde{r}}\vec{e_{\tilde{r}}} + \frac{1}{\tilde{r}}\frac{\partial \tilde{T}\left(\tilde{r},\tilde{t}\right)}{\partial \tilde{\varphi}}\vec{e_{\tilde{\varphi}}} + \frac{\partial \tilde{T}\left(\tilde{r},\tilde{t}\right)}{\partial \tilde{z}}\vec{e_{\tilde{z}}}$ therefore,

$$grad\tilde{T}\left(\tilde{r},\tilde{t}\right)=\frac{\partial\tilde{T}\left(\tilde{r},\tilde{t}\right)}{\partial\tilde{r}}\vec{e}_{\tilde{r}}. \tag{9}$$

Along with all of the equations above, we consider the initial-boundary conditions

$$\begin{aligned}&\tilde{u}\left(\tilde{r},0\right)=0,\ \tilde{T}\left(\tilde{r},0\right)=\tilde{T}_\infty,\ \tilde{q}\left(\tilde{r},0\right)=0,\ \tilde{r}\in\left[R_0,\infty\right),\\&\tilde{u}\left(R_0,\tilde{t}\right)=0,\ \tilde{T}\left(R_0,\tilde{t}\right)=\tilde{T}_\infty+\tilde{T}_\infty f_1\left(\tilde{t}\right),\ \tilde{t}>0,\\&\tilde{u}\left(\tilde{r},\tilde{t}\right)\to 0,\ T\left(\tilde{r},\tilde{t}\right)\to\tilde{T}_\infty \text{ as } \tilde{r}\to\infty.\end{aligned} \tag{10}$$

In the above relations function $f_1(\tilde{t})$ is a piecewise function of exponential order to infinity. Using the following dimensionless parameters and functions,

$$\begin{aligned}&r=\frac{\tilde{r}}{R_0},\ t=\frac{v\tilde{t}}{R_0^2},\ u=\frac{R_0\tilde{u}}{v},\ T=\frac{\tilde{T}-\tilde{T}_\infty}{\tilde{T}_\infty},\ q=\frac{R_0\tilde{q}}{k\tilde{T}_\infty},\ Gr=\frac{g\beta\tilde{T}_\infty R_0^3}{v^2},\\&H_a=B_0R_0\sqrt{\frac{\sigma}{\mu}},\ \tau=\frac{v\tau_q}{R_0^2},\ \Pr=\frac{\mu c_p}{k},\ f\left(t\right)=f_1\left(\frac{R_0^2 t}{v}\right),\end{aligned} \tag{11}$$

we obtain the non-dimensional equations:

$$\frac{\partial u}{\partial t}=\left(1+\frac{1}{\gamma}\right)\frac{1}{r}\frac{\partial}{\partial r}\left(r\frac{\partial u}{\partial r}\right)+GrT-H_a^2u \tag{12}$$

$$q+\tau\frac{\partial q}{\partial t}=-\frac{\partial T}{\partial r} \tag{13}$$

$$\Pr\frac{\partial T}{\partial t}=-\frac{1}{r}\frac{\partial}{\partial r}\left(rq\right) \tag{14}$$

The non-dimensional forms of Eq. (10) are

$$u(r,0)=0,\ T\left(r,0\right)=0,\ q\left(r,0\right)=0,\ r\in\left[1,\infty\right), \tag{15}$$

$$u\left(1,t\right)=0,\ T\left(1,t\right)=f\left(t\right),\ \lim_{r\to\infty}u\left(r,t\right)=0,\ \lim_{r\to\infty}T\left(r,t\right)=0 \tag{16}$$

3. The Generalized Fractional Mathematical Model

In this paper, we consider a generalized Cattaneo's law given by the constitutive equation of the thermal flux,

$$q(r,t)+\tau\,{}_{C}D_{t}^{\alpha}q(r,t)=-\frac{\partial T(r,t)}{\partial r},\ \alpha\in(0,1] \tag{17}$$

where $D_{t}^{\alpha}q(r,t)$ denotes Caputo time-fractional derivative operator defined as

$${}_{C}D_{t}^{\alpha}q(r,t)=\begin{cases}\dfrac{1}{\Gamma(1-\alpha)}\displaystyle\int_{0}^{t}(t-\sigma)^{-\alpha}\,\dot{q}(r,\sigma)d\sigma,\ 0\le\alpha<1,\\ \dfrac{\partial q(r,t)}{\partial t}=\dot{q}(r,t),\ \alpha=1.\end{cases} \tag{18}$$

Let ${}_{C}h(\alpha,t)$ be the Caputo kernel given by

$${}_{c}h(\alpha,t)=\frac{t^{-\alpha}}{\Gamma(1-\alpha)},\ 0\le\alpha<1. \tag{19}$$

Using Eq. (18) and Eq. (19), the time-fractional Caputo derivative is written as a convolution, namely,

$${}_{C}D_{t}^{\alpha}q(r,t)={}_{C}h(r,t)*\frac{\partial q(r,t)}{\partial t}. \tag{20}$$

Applying Laplace transform on Eq. (18) to Eq. (20), we obtain

$$\begin{gathered}L\left\{{}_{C}D_{t}^{\alpha}q(r,t)\right\}=L\left\{{}_{C}h(r,t)\right\}.L\left\{\frac{\partial q(r,t)}{\partial t}\right\}=\frac{1}{s^{1-\alpha}}\left[sL\left\{q(x,t)\right\}-q(r,0)\right]=\\ s^{\alpha}\hat{q}(r,s)-s^{\alpha-1}q(r,0),\ \alpha\in[0,1],\end{gathered} \tag{21}$$

where $\hat{q}(r,s)=L\left\{q(r,t)\right\}=\int_{0}^{\infty}q(r,t)e^{-st}dt$ denotes the Laplace transform of function $q(r,t)$.

4. Solution of the Generalized Mathematical Model

The solutions of the proposed problem are obtained by using Laplace transform and Bessel functions.

4.1 Solution of the Generalized Thermal Process

In this section, we find the solution of the Eq. (14) and Eq. (17) along with the initial and boundary conditions

$$T(r,0)=0,\ q(r,0)=0 \tag{22}$$

$$T(1,t)=f(t),\ \lim_{r\to\infty}T(r,t)=0,\ t>0. \tag{23}$$

Applying the Laplace transform to Eq. (14) and Eq. (17) and using Eq. (21) and Eq. (22), we obtain the transformed equations

$$\Pr s\hat{T}(r,s) = -\frac{1}{r}\frac{\partial}{\partial r}\left(r\hat{q}\left(r,s\right)\right) \tag{24}$$

$$\left(1+\tau s^{\alpha}\right)\hat{q}(r,s) = -\frac{\partial \hat{T}\left(r,s\right)}{\partial r} \tag{25}$$

The Laplace transform $\hat{T}\left(r,s\right)$ has to satisfy the boundary conditions

$$\hat{T}\left(1,s\right) = \hat{f}\left(s\right),\ \lim_{r\to\infty}\hat{T}\left(r,s\right) = 0. \tag{26}$$

Eliminating $\hat{q}\left(r,s\right)$ between Eq. (24) and Eq. (25) we have that $\hat{T}\left(r,s\right)$ satisfies the differential equation

$$\theta\left(s\right)\hat{T}\left(r,s\right) = \frac{1}{r}\frac{\partial}{\partial r}\left(r\frac{\partial \hat{T}\left(r,s\right)}{\partial r}\right), \tag{27}$$

where

$$\theta\left(s\right) = \Pr s\left(1+\tau s^{\alpha}\right). \tag{28}$$

Eq. (27) is written in the equivalent form

$$r^{2}\frac{\partial^{2}\hat{T}\left(r,s\right)}{\partial r^{2}} + \frac{\partial \hat{T}\left(r,s\right)}{\partial r} - \left(r\sqrt{\theta\left(s\right)}\right)^{2}\hat{T}\left(r,s\right) = 0. \tag{29}$$

that is a modified Bessel equation with the general solution [18,19],

$$\hat{T}\left(r,s\right) = A\left(s\right)I_{0}\left(r\sqrt{\theta\left(s\right)}\right)^{2} + B\left(s\right)K_{0}\left(r\sqrt{\theta\left(s\right)}\right), \tag{30}$$

where $I_{0}\left(z\right)$, $K_{0}\left(z\right)$ are the modified Bessel functions of the first and second kind of order zero, and $A\left(s\right)$, $B\left(s\right)$ will be determined from the boundary conditions.

Since $\lim_{r\to\infty} I_{0}\left(r\sqrt{\theta\left(s\right)}\right) = +\infty$ and $\lim_{r\to\infty} K_{0}\left(r\sqrt{\theta\left(s\right)}\right) = 0$, we must consider $A\left(s\right) = 0$ in order to have a finite temperature for $r \to \infty$. Now, using the second boundary condition Eq. (27), we obtain the following form of the transformed temperature:

$$\hat{T}\left(r,s\right) = \hat{f}\left(s\right)\frac{K_{0}\left(r\sqrt{\theta\left(s\right)}\right)}{K_{0}\left(\sqrt{\theta\left(s\right)}\right)}. \tag{31}$$

The inverse Laplace transform of function Eq. (31) cannot be obtained in a simple analytical form, hence, the numerical values of the temperature $T(r,t)=L^{-1}\{\hat{T}(r,s)\}$ are determined by using the Stehfest's algorithm. According to Stehfest's algorithm, the temperature is approximated by

$$T(r,t)\simeq\frac{\ln 2}{t}\sum_{j=1}^{2n}D_j\hat{T}\left(r,j\frac{\ln 2}{t}\right), \tag{32}$$

where

$$D_j=(-1)^{j+n}\sum_{i=\left[\frac{j+1}{2}\right]}^{\min(j,n)}\frac{i^n(2i)!}{(n-i)!i!(i-1)!(j-i)!(2i-j)!}. \tag{33}$$

In the above relations, $[x]$ denotes the integer part of $x\in\mathbb{R}$, and n is an integer positive number.

Let's note that for $\alpha\in(0,1)$ and $\tau>0$, the solutions Eq. (31) and Eq. (32) give the temperature field corresponding to the generalized fractional Cattaneo thermal process. When $\alpha=1$ and $\tau>0$, Eq. (32) give the temperature of the classical Cattaneo thermal process.

5. Fluid Velocity

The fluid velocity is given by the solution of differential Eq. (12) along with the initial and boundary conditions Eq. (15) and Eq. (16).

Applying the Laplace transform to Eq. (12), using the initial condition (15), and the expression (31) of the temperature we obtain the following equation of the transformed velocity $\hat{u}(r,s)$:

$$\frac{\partial^2\hat{u}(r,s)}{\partial r^2}+\frac{1}{r}\frac{\partial\hat{u}(r,s)}{\partial r}-\frac{s+Ha^2}{\gamma_0}\hat{u}(r,s)+\frac{Gr}{\gamma_0}\hat{f}(s)\frac{K_0\left(r\sqrt{\theta(s)}\right)}{K_0\left(\sqrt{\theta(s)}\right)},\ \gamma_0=1+\frac{1}{\gamma}. \tag{34}$$

A particular solution of Eq. (34) in given by

$$\hat{u}_p(r,s)=-\frac{Gr\hat{f}(s)}{\gamma_0\theta(s)-s-Ha^2}.\frac{K_0\left(r\sqrt{\theta(s)}\right)}{K_0\left(\sqrt{\theta(s)}\right)} \tag{35}$$

The homogenous equation associated with Eq. (34) is the modified Bessel equation

$$r^2\frac{\partial^2\hat{u}}{\partial r^2}+r\frac{\partial\hat{u}}{\partial r}-\left(r\sqrt{\frac{s+Ha^2}{\gamma_0}}\right)^2\hat{u}=0. \tag{36}$$

whose general solution is

$$\hat{u}_h(r,s)=C(s)I_0\left(r\sqrt{\varphi(s)}+D(s)K_0r\sqrt{\varphi(s)}\right), \tag{37}$$

where $\varphi(s)=\dfrac{s+Ha^2}{\gamma_0}$.

To have the finite velocity for $r\to\infty$, we must take $C(s)=0$. The general solution of Eq. (34) is

$$\hat{u}(r,s)=D(s)K_0\left(r\sqrt{\varphi(s)}+M(s)K_0 r\sqrt{\varphi(s)}\right), \tag{38}$$

where $M(s)=-\dfrac{Gr\,\hat{f}(s)}{\left[\gamma_0\theta(s)-s-Ha^2\right]K_0\left(\sqrt{\theta(s)}\right)}$.

Using the boundary condition $\hat{u}(1,s)=0$, we have

$$D(s)=-\frac{M(s)K_0\left(\sqrt{\theta(s)}\right)}{K_0\left(\sqrt{\varphi(s)}\right)}=\frac{Gr\,\tilde{f}(s)}{\left[\gamma_0\theta(s)-s-Ha^2\right]K_0\left(\sqrt{\varphi(s)}\right)}. \tag{39}$$

The transformed velocity field is given by

$$\hat{u}(r,s)=\frac{Gr\,\hat{f}(s)}{\left[\gamma_0\theta(s)-s-Ha^2\right]}\left[\frac{K_0\left(r\sqrt{\varphi(s)}\right)}{K_0\left(\sqrt{\varphi(s)}\right)}-\frac{K_0\left(r\sqrt{\theta(s)}\right)}{K_0\left(\sqrt{\theta(s)}\right)}\right]. \tag{40}$$

The numerical values of the velocity field in the real domain are obtained using the Stehfest's algorithm, namely,

$$u(r,t)\simeq\frac{\ln 2}{t}\sum_{j=1}^{2n}D_j\hat{u}\left(x,\,j\frac{\ln 2}{t}\right), \tag{41}$$

where D_j is given by Eq. (33).

6. Numerical Results and Discussions

In this section, the obtained exact solutions are studied numerically in order to determine the effects of temperature and velocity. The generalized mathematical model of thermal transport can be particularized to obtain the classical Cattaneo' law, when the memory parameter is $\alpha=1$. Figure 2 shows the variation of the dimensionless temperature $T(r,t)$, for small values of time and for different values of the fractional parameter α. The temperature profiles were drawn for two cases corresponding to the fractional mathematical model but also for the classic of thermal transport Cattaneo. As expected, the fractional Catteno heat transfer model generates higher temperature than the classic Cattaneo model. It is noted that the weight function that affects the temperature gradient in the case of the classic Cattaneo model is $k_1(t)=\exp(-t/\tau)$, while in the fractional Cattaneo model it is $k_2(t)=t^{\alpha-1}E_{\alpha,\alpha}(-t^{\alpha}/\tau)$, where $E_{\alpha,\beta}(\cdot)$ is two-parameters Mittage-Leffler function. Obviously $\lim_{\alpha \to 1} k_2(t) = k_1(t)$ where it is visible in Figure 2 because the temperature is close to that corresponding to $\alpha = 1$ when $\alpha = 0.9$. The influence of the thermal relaxation time on the thermal field is shown in figure 3. It is shown that the temperature decreases with the increasing of relaxation time τ.

Figure 4 shows the influence of the Grashof number on the fluid motion. It is seen that the fluid velocity increases with the increasing of Grashof number. Noted that the increasing value of Grashof number leads to increase in buoyancy factor of the fluid.

Fluid motion is numerically analysed by the graph shown in Figure 5 where the graphs show the velocity profile versus the radial variable r with different values of the fractional parameter α. It is observed that there is a perfect correlation between the evolution of fluid temperature and velocity concerning the α namely memory parameter, the velocity values decrease with the memory parameter α. This is due to the fact that the velocity has a maximum value near the cylindrical surface and tends to zero away from it.

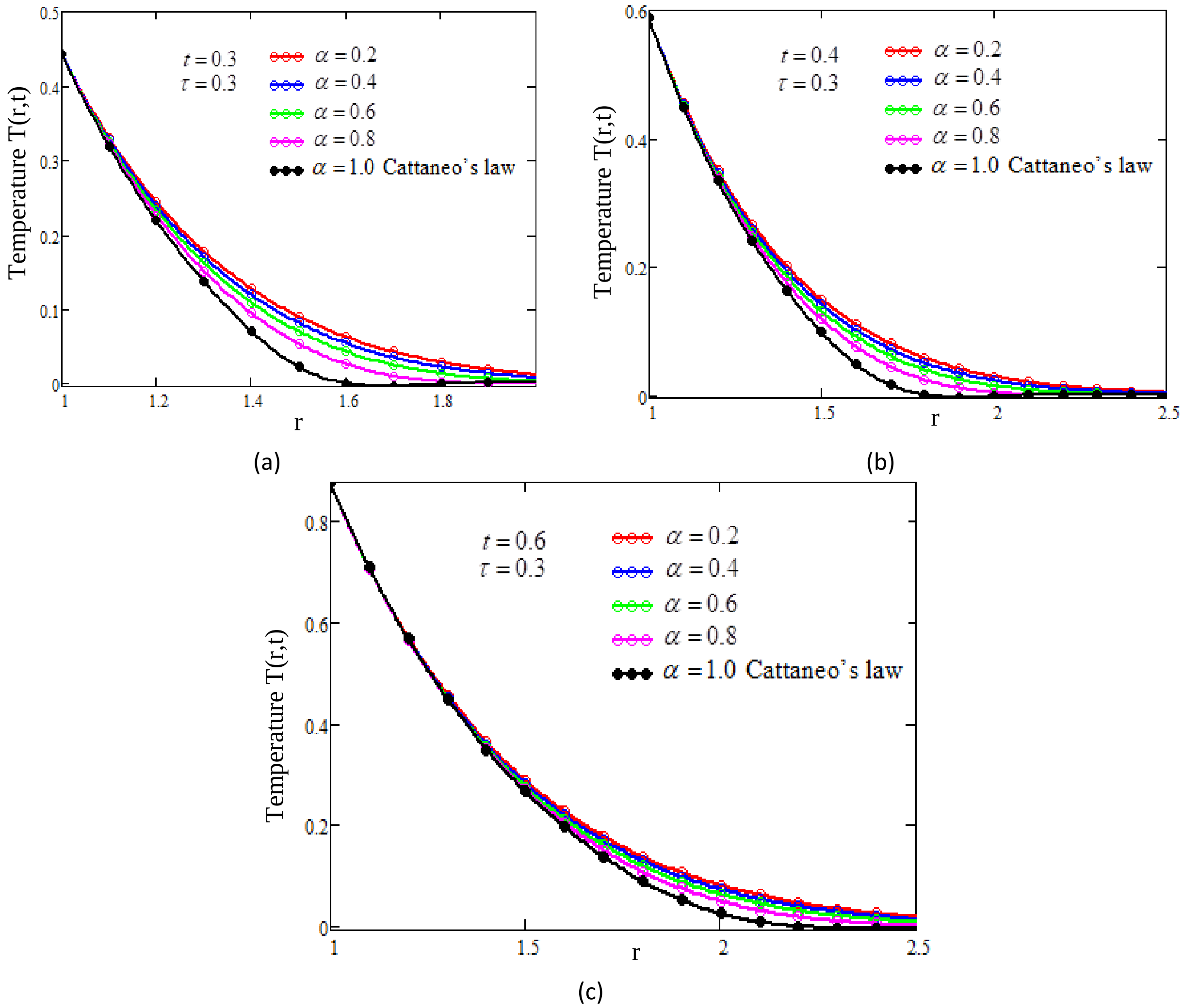

Fig. 2. The profiles of the nondimensional temperature $T(r,t)$ for different values of fractional parameter

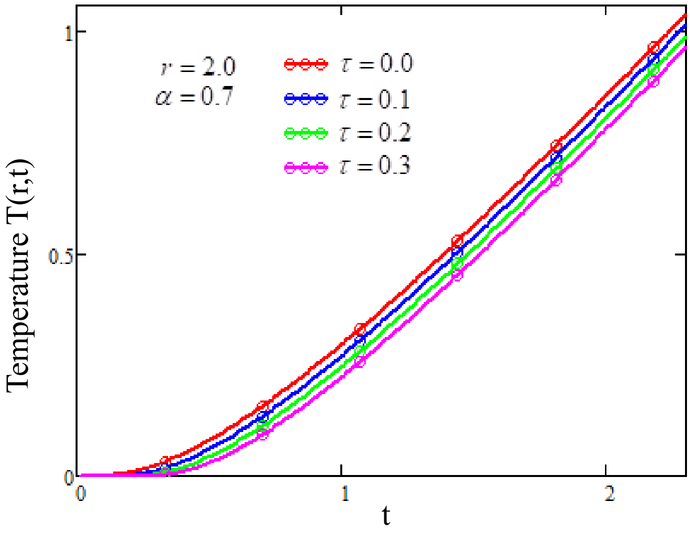

(a)

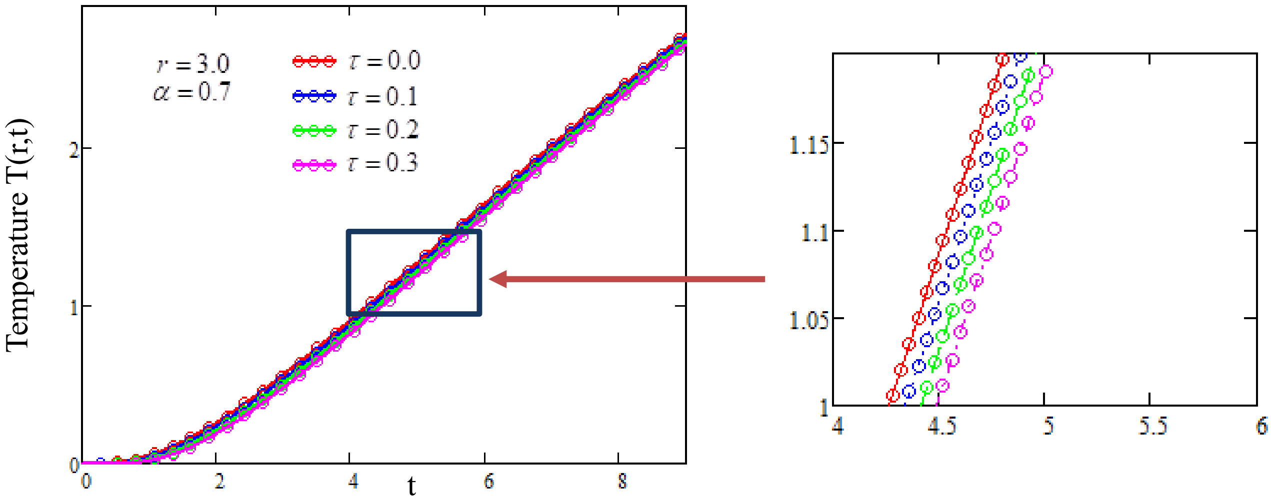

(b)

Fig. 3. The influence of the thermal relaxation time τ on the temperature field

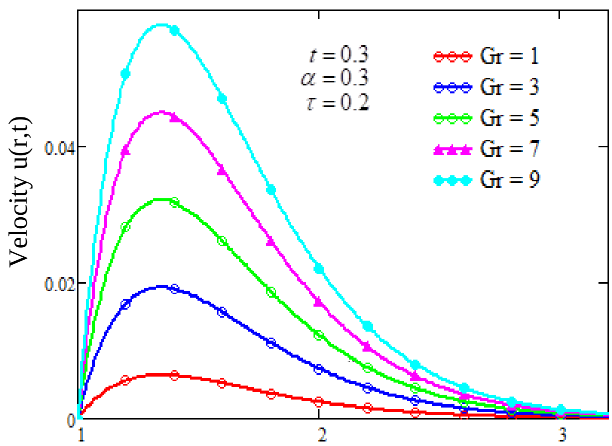

(a)

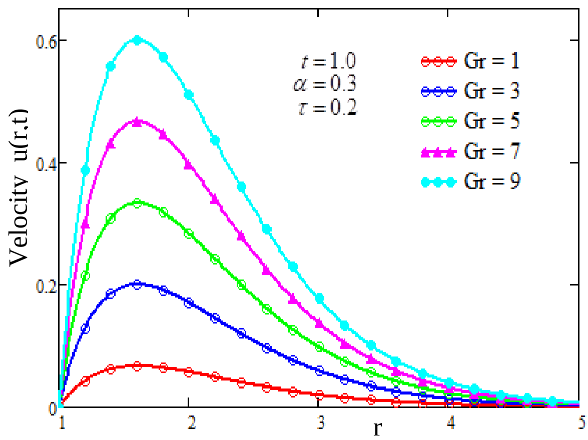

(b)

CFD Letters
Volume 14, Issue 12 (2022) 38-51

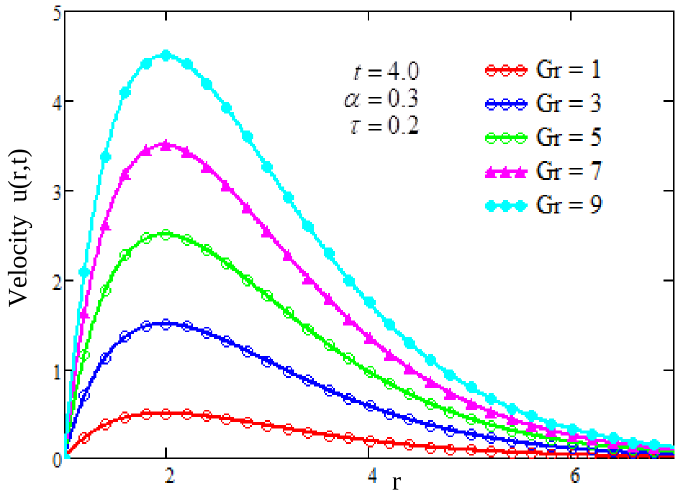

(c)

Fig. 4. The influence of Grashof number Gr on the fluid velocity

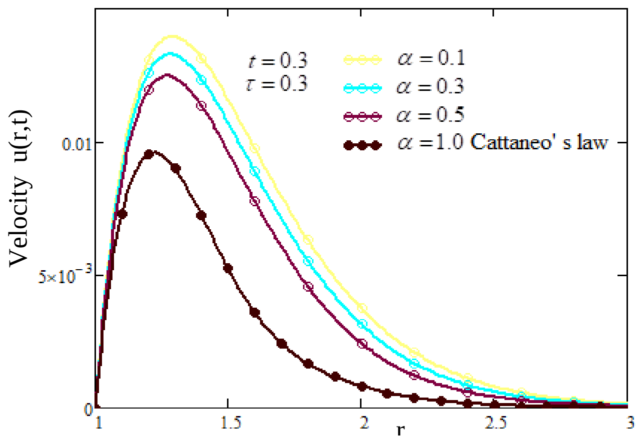

(a)

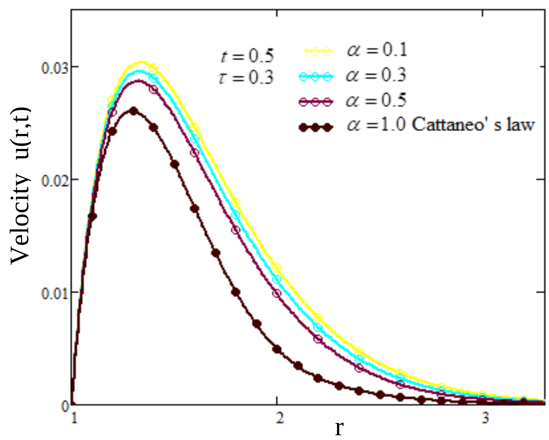

(b)

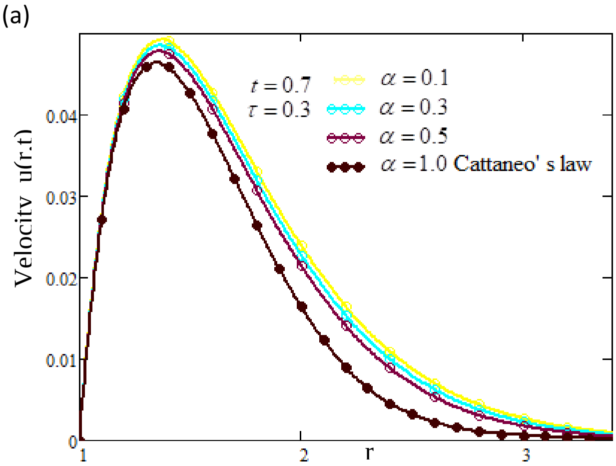

(c)

Fig. 5. Velocity profiles $u(r,t)$ versus r for the different values of the fractional parameter α

7. Conclusion

In this paper, we have investigated the unsteady axial symmetric flows of incompressible and electrically conducting Casson fluids over a vertical cylinder with time-variable temperature, under influence of an external transversely magnetic field. The thermal transport is described by a generalized mathematical model based on the time-fractional differential equation of Cattaneo's law with Caputo derivative. Based on the model, we can obtain the effect of temperature gradient history on heat transport and fluid motion. The main observations in summarized form are listed as:

I. The fractional Cattaneo heat transfer model generates higher temperature than the classic Cattaneo model and for $\alpha = 0.9$ the temperature profile is close to that corresponding to $\alpha = 1$.
II. The decreasing change in temperature is noted for the increasing value of relaxation time τ.
III. The fluid velocity increases with the increasing of Grashof number. Noted that the increasing value of Grashof number leads to increase in buoyancy factor of the fluid.
IV. There is a perfect correlation between the evolution of fluid temperature and velocity concerning the α namely memory parameter, the velocity values decrease with the memory parameter α due to the fact that the velocity has a maximum value near the cylindrical surface and tends to zero away from it.

Acknowledgement
The authors would like to acknowledge Universiti Malaysia Pahang (UMP) for the financial support via vote number RDU213207 and Post Graduate Research Scheme (PGRS210329) for this research.

References

[1] Asogwa, K. K., and A. A. Ibe. "A study of MHD Casson fluid flow over a permeable stretching sheet with heat and mass transfer." *Journal of Engineering Research and Reports* 16, no. 2 (2020): 10-25. https://doi.org/10.9734/jerr/2020/v16i217161
[2] Abdullahi, Faruk, Ibrahim Haliru Wala, and Muhammad Abdurrahman Sani. "Casson Fluid Flow Effects on MHD Unsteady Heat And Mass Transfer Free Convective Past An Infinite Vertical Plate." *International Journal of Scientific and Research Publications* 10, no. 11 (2020): 104-118. https://doi.org/10.29322/IJSRP.10.11.2020.p10712
[3] Mondal, Razon K., Partha P. Gharami, Sarder F. Ahmmed, and S. M. Arifuzzaman. "A simulation of Casson fluid flow with variable viscosity and thermal conductivity effects." *Mathematical Modelling of Engineering Problems* 6, no. 4 (2019): 625-633. https://doi.org/10.18280/mmep.060418
[4] Aghighi, Mohammad Saied, Amine Ammar, Christel Metivier, and M. Gharagozlu. "Rayleigh-Bénard convection of Casson fluids." *International Journal of Thermal Sciences* 127 (2018): 79-90. https://doi.org/10.1016/j.ijthermalsci.2018.01.016
[5] Parandhamaa, A., K. V. S. Rajua, and M. Changal Rajub. "MHD Casson fluid flow through a vertical plate." *Journal of Computational & Applied Research in Mechanical Engineering (JCARME)* 9, no. 2 (2020): 343-350.
[6] Ramanuja, M., and V. Nagaradhika. "MHD Analysis of Casson Fluid Through a Vertical Porous Surface with Chemical Reaction." *Global Scientific Journals* 8, no. 4 (2020): 469-482.
[7] Kumar, Gaurav, and S. M. K. Rizvi. "Casson fluid flow past on vertical cylinder in the presence of chemical reaction and magnetic field." *Applications and Applied Mathematics: An International Journal (AAM)* 16, no. 1 (2021): 524-537.
[8] Ali, M. E., and N. Sandeep. "Cattaneo-Christov model for radiative heat transfer of magnetohydrodynamic Casson-ferrofluid: A numerical study." *Results in Physics* 7 (2017): 21-30. https://doi.org/10.1016/j.rinp.2016.11.055
[9] Yusof, Nur Syamila, Siti Khuzaimah Soid, Mohd Rijal Illias, Ahmad Sukri Abd Aziz, and Nor Ain Azeany Mohd Nasir. "Radiative Boundary Layer Flow of Casson Fluid Over an Exponentially Permeable Slippery Riga Plate with Viscous Dissipation." *Journal of Advanced Research in Applied Sciences and Engineering Technology* 21, no. 1 (2020): 41-51. https://doi.org/10.37934/araset.21.1.4151
[10] Aman, Sidra, Syazwani Mohd Zokri, Zulkhibri Ismail, Mohd Zuki Salleh, and Ilyas Khan. "Effect of MHD and porosity on exact solutions and flow of a hybrid Casson-nanofluid." *Journal of Advanced Research in Fluid Mechanics and Thermal Sciences* 44, no. 1 (2018): 131-139.
[11] Omar, Nur Fatihah Mod, Husna Izzati Osman, Ahmad Qushairi Mohamad, Rahimah Jusoh, and Zulkhibri Ismail. "Effects of radiation and magnetohydrodynamic on unsteady Casson fluid over accelerated plate." *Journal of Advanced Research in Fluid Mechanics and Thermal Sciences* 85, no. 1 (2021): 93-100. https://doi.org/10.37934/arfmts.85.1.93100

[12] Daud, Marjan Mohd, Lim Yeou Jiann, Sharidan Shafie, and Rahimah Mahat. "Casson Fluid Convective Flow in an Accelerated Microchannel with Thermal Radiation using the Caputo Fractional Derivative." *CFD Letters* 14, no. 8 (2022): 12-19. https://doi.org/10.37934/cfdl.14.8.1219
[13] Guo, Bing, Ali Raza, Kamel Al-Khaled, Sami Ullah Khan, Saadia Farid, Ye Wang, M. Ijaz Khan, M. Y. Malik, and S. Saleem. "Fractional-order simulations for heat and mass transfer analysis confined by elliptic inclined plate with slip effects: A comparative fractional analysis." *Case Studies in Thermal Engineering* 28 (2021): 101359. https://doi.org/10.1016/j.csite.2021.101359
[14] Ogunrinde, R. B., U. K. Nwajeri, S. E. Fadugba, R. R. Ogunrinde, and K. I. Oshinubi. "Dynamic model of COVID-19 and citizens reaction using fractional derivative." *Alexandria Engineering Journal* 60, no. 2 (2021): 2001-2012. https://doi.org/10.1016/j.aej.2020.09.016
[15] Zhang, Qiao, Yuxin Sun, and Jialing Yang. "Bio-heat transfer analysis based on fractional derivative and memory-dependent derivative heat conduction models." *Case Studies in Thermal Engineering* 27 (2021): 101211. https://doi.org/10.1016/j.csite.2021.101211
[16] Thakare, Shivcharan, and M. S. Warbhe. "Time fractional heat transfer analysis in thermally sensitive functionally graded thick hollow cylinder with internal heat source and its thermal stresses." In *Journal of Physics: Conference Series*, vol. 1913, no. 1, p. 012112. IOP Publishing, 2021. https://doi.org/10.1088/1742-6596/1913/1/012112
[17] Xu, Guangying, and Jinbao Wang. "Analytical solution of time fractional Cattaneo heat equation for finite slab under pulse heat flux." *Applied Mathematics and Mechanics* 39, no. 10 (2018): 1465-1476. https://doi.org/10.1007/s10483-018-2375-8
[18] Qi, Hai-Tao, Huan-Ying Xu, and Xin-Wei Guo. "The Cattaneo-type time fractional heat conduction equation for laser heating." *Computers & Mathematics with Applications* 66, no. 5 (2013): 824-831. https://doi.org/10.1016/j.camwa.2012.11.021
[19] Han, Shihao, Liancun Zheng, Chunrui Li, and Xinxin Zhang. "Coupled flow and heat transfer in viscoelastic fluid with Cattaneo-Christov heat flux model." *Applied Mathematics Letters* 38 (2014): 87-93. https://doi.org/10.1016/j.aml.2014.07.013
[20] Hema, M., and I. S. Shivakumara. "Impact of Cattaneo law of heat conduction on an anisotropic Darcy-Bénard convection with a local thermal nonequilibrium model." *Thermal Science and Engineering Progress* 19 (2020): 100620. https://doi.org/10.1016/j.tsep.2020.100620